

Identification and Recovery of Injective Transforms

Adnan A. Y. Mustafa

Department of Mechanical and Industrial Engineering, Kuwait University, P. O. Box 5969 - Safat
Kuwait 13060, E-mail: symymus@kuc01.kuniv.edu.kw

Abstract

Image transforms are used extensively in image processing to convert one image form into another form. These transforms are either point-operation transforms or neighborhood-operation transforms. Injective transforms, also known as reversible or one-to-one transforms, are a subset of point-operation transforms where each intensity value maps to a distinct intensity value. In this paper we present a novel technique that can identify if an image was processed by an injective transform. The injective mapping is also recovered in the process. The technique is applicable to both linear and non-linear transforms. We introduce two measures that assess the degree of injective mapping and the degree of functional mapping of the transform. The technique is based on the attributes of the image variation number which is an entropy-similar informative measure. Tests are conducted on real images to show the validity of our technique.

Index Terms: Image transforms, Injective transforms, transform recovery, image information, image restoration

1. Introduction

Image transforms play an important role in image processing and image analysis [1] [2] [3]. They are used extensively to convert an image into a (more meaningful) new form of the image. These transforms are either neighborhood-operation transforms or point-operation transforms. Neighborhood-operation transforms (or local transforms) perform their transform operation based on the neighborhood of a pixel. Examples of these transforms are edge filters (e.g. Roberts, Sobel), low-pass filters, high-pass filters and local entropy [4]. Point-operation transforms (also known as gray-scale or pixel brightness transformations) perform their transform operation based entirely on the corresponding pixel value in the input image. Examples of point-operation transforms are image equalization, image contrast enhancement, image inversion and image thresholding. They are also used to correct for digitizer or display device limitations such as non-linearity [5]. Injective [6] (one-to-one) transforms are a subset of point-operation transforms where each

intensity value maps to a distinct intensity value. If \mathfrak{S} represents the injective transform then,

$$\mathfrak{S}^{-1}(\mathfrak{S}(u)) = u \quad (1)$$

where u is the intensity level. Hence, these transforms are reversible. Examples of Injective transforms are image equalization and image inversion. In this paper we present a novel technique that can identify if an image was processed by an injective transform. Regardless of the complexity of the injective transform, such as a random injective transform mapping, the transform can be easily identified with the technique. The technique is applicable to both linear and non-linear transforms. The injective mapping function is also recovered in the process. The technique is based on the attributes of the image variation number, a new entropy-similar information measure that has many applications in image analysis [7]. Two measures that assess the degree of injective mapping and the degree of functional mapping of the transform are introduced. This paper is divided into five sections as follows: section 2 follows this introduction with a presentation of the image variation number, its attributes and its relation to entropy, section 3 presents injective transforms and the method by which an injective transform is identified and recovered, the results of our tests are presented in section 4, and the paper concludes with section 5.

2. The Image Variation Number

The Image Variation Number (Π) measures the amount of information of an image. For an image \mathbf{x} , $\Pi(\mathbf{x})$ is defined as the number of non-zero elements of the image histogram or the number of unique intensity gray-scale values in image \mathbf{x} ,

$$\Pi(\mathbf{x}) = \sum_{i=0}^{L-1} \delta(h_i(\mathbf{x})) \quad (2)$$

where δ is the kronecker-delta function,

$$\delta(x) = \begin{cases} 1 & \text{if } x > 0 \\ 0 & \text{otherwise} \end{cases} \quad (3)$$

and $h_i(\mathbf{x})$, $i = 0, \dots, L-1$, denotes the normalized image intensity histogram. $L = 2^n$ is the number of gray levels in

the image, where n is the number of bits used to represent the image. Obviously an image with many distinct gray-scale values clearly contains more information than an image with a lesser number of distinct gray-scale values. $\Pi(\mathbf{x})$ is bounded by, $1 \leq \Pi(\mathbf{x}) \leq L$, or, $0 \leq \log_2(\Pi(\mathbf{x})) \leq n$.

2.1. The Image Variation Number and Entropy

The Image variation number is related to the image entropy (E),

$$E(\mathbf{x}) = - \sum_{i=0}^{L-1} h_i(\mathbf{x}) \log_2(h_i(\mathbf{x})) \quad (4)$$

Since, only the non-zero elements of the histogram actually contribute to the entropy, we can restate the entropy equation as,

$$E(\mathbf{x}) = - \sum_{i=0, h_i \neq 0}^{L-1} h_i(\mathbf{x}) \log_2(h_i(\mathbf{x})) \quad (5)$$

Using the *Log Sum Inequality* from information theory [8], we obtain,

$$\sum_{i=0, h_i \neq 0}^{L-1} h_i(\mathbf{x}) \log_2(h_i(\mathbf{x})) \geq \left(\sum_{i=0, h_i \neq 0}^{L-1} h_i(\mathbf{x}) \right) \log_2 \left(\frac{\sum_{i=0, h_i \neq 0}^{L-1} h_i(\mathbf{x})}{\sum_{i=0, h_i \neq 0}^{L-1} 1} \right) \quad (6)$$

But,

$$\Pi(\mathbf{x}) = \sum_{i=0}^{L-1} \delta(h_i(\mathbf{x})) = \sum_{i=0, h_i \neq 0}^{L-1} 1 \quad (7)$$

$$\sum_{i=0, h_i \neq 0}^{L-1} h_i(\mathbf{x}) = \sum_{i=0}^{L-1} h_i(\mathbf{x}) = 1 \quad (8)$$

Hence, we obtain,

$$\sum_{i=0, h_i \neq 0}^{L-1} h_i(\mathbf{x}) \log_2(h_i(\mathbf{x})) \geq \log_2 \left(\frac{1}{\Pi(\mathbf{x})} \right) \quad (9)$$

or,

$$E(\mathbf{x}) \leq \log_2(\Pi(\mathbf{x})) \quad (10)$$

The last equation states that the log of the intensity variation number is always larger than (or at best equal to) the image entropy. As a result, $0 \leq E(\mathbf{x}) \leq \log_2(\Pi(\mathbf{x})) \leq n$. Thus knowledge of the image variation number results in knowledge of an upper limit ($\leq n$) on image entropy. Conversely, knowledge of the image entropy results in knowledge of a lower bound on the image variation number.

2.2. The Joint Image Variation Number

The joint variation number between two images \mathbf{x}_1 and \mathbf{x}_2 ,

$\Pi(\mathbf{x}_1, \mathbf{x}_2)$, is defined as the number of non-zero elements of the joint histogram distribution of \mathbf{x}_1 and \mathbf{x}_2 , i.e.,

$$\Pi(\mathbf{x}_1, \mathbf{x}_2) = \sum_{i=0}^{L-1} \sum_{j=0}^{L-1} \delta(h_{ij}(\mathbf{x}_1, \mathbf{x}_2)) \quad (11)$$

where $h_{ij}(\mathbf{x}_1, \mathbf{x}_2)$, $i = 0 \dots L-1$, $j = 0 \dots L-1$, denotes the normalized joint histogram distributions of images \mathbf{x}_1 and \mathbf{x}_2 . $L = 2^n$ is the number of gray levels in the image, where n is the number of bits used to represent the image. Both image vectors \mathbf{x}_1 and \mathbf{x}_2 are of size K . Furthermore, $\Pi(\mathbf{x}_1, \mathbf{x}_2)$ is bounded by a lower and an upper bound, $l_1 \leq \Pi(\mathbf{x}_1, \mathbf{x}_2) \leq l_2$. The lower bound, $l_1 = \max(\Pi(\mathbf{x}_1), \Pi(\mathbf{x}_2))$, is the maximum number of distinct gray-scale values of the two images, which can not exceed 2^n . The upper bound, l_2 , is the size of the image vector (K), or the entire number of possible intensity combinations, 2^{2n} , whichever is smaller,

$$1 \leq \max(\Pi(\mathbf{x}_1), \Pi(\mathbf{x}_2)) \leq \Pi(\mathbf{x}_1, \mathbf{x}_2) \leq \min(2^{2n}, K) \quad (12)$$

Note that the joint image variation number can be extended to more than two images [7].

2.3. The Joint Image Variation Number and Joint Image Entropy

The joint image variation number of two images \mathbf{x}_1 and \mathbf{x}_2 , $\Pi(\mathbf{x}_1, \mathbf{x}_2)$, is related to their joint image entropy, $E(\mathbf{x}_1, \mathbf{x}_2)$. Let $E(\mathbf{x}_1, \mathbf{x}_2)$ be given by,

$$E(\mathbf{x}_1, \mathbf{x}_2) = - \sum_{i=0}^{L-1} \sum_{j=0}^{L-1} h_{ij}(\mathbf{x}_1, \mathbf{x}_2) \log_2(h_{ij}(\mathbf{x}_1, \mathbf{x}_2)) \quad (13)$$

Since, only the non-zero elements of the histogram contribute to the image entropy, the above equation can be rewritten as,

$$\underbrace{\sum_{i=0}^{L-1} \sum_{j=0}^{L-1} h_{ij}(\mathbf{x}_1, \mathbf{x}_2) \log_2(h_{ij}(\mathbf{x}_1, \mathbf{x}_2))}_{h_{ij}(\mathbf{x}_1, \mathbf{x}_2) \neq 0} \geq \log_2 \left(\frac{1}{\Pi(\mathbf{x}_1, \mathbf{x}_2)} \right) \quad (14)$$

Using the *Log Sum Inequality* as before, we obtain,

$$E(\mathbf{x}_1, \mathbf{x}_2) = - \underbrace{\sum_{i=0}^{L-1} \sum_{j=0}^{L-1} h_{ij}(\mathbf{x}_1, \mathbf{x}_2) \log_2(h_{ij}(\mathbf{x}_1, \mathbf{x}_2))}_{h_{ij}(\mathbf{x}_1, \mathbf{x}_2) \neq 0} \quad (15)$$

which produces,

$$E(\mathbf{x}_1, \mathbf{x}_2) \leq \log_2(\Pi(\mathbf{x}_1, \mathbf{x}_2)) \quad (16)$$

i.e. the joint image entropy of two images is always smaller than (or at best equal to) the log of the joint image

variation number. This implies that the joint image entropy has the following upper limit,

$$0 \leq E(\mathbf{x}_1, \mathbf{x}_2) \leq \log_2(\Pi(\mathbf{x}_1, \mathbf{x}_2)) \leq$$

$$\log_2(\Pi(\mathbf{x}_1) \cdot \Pi(\mathbf{x}_2)) \leq \log_2(\min(2^{2n}, K)) \quad (17)$$

An interpretation of the joint variation number of two images is that it is the number of non-zero elements of the gray-scale correspondence table (*GCT*) which is a binary table that indicates the gray-scale intensity mapping between two images.

3. Injective Transforms

As earlier stated, point-operation transforms modify an image by changing the gray-scale intensity values of each pixel to a new value, by some intensity mapping function. Any pixel in the output image depends exclusively on the corresponding input pixel intensity, $x_o(r, c) = f(x_i(r, c))$, where $x_o(r, c)$ and $x_i(r, c)$ are the output and input images, respectively, and f is the mapping function. If f is a linear function, f_L , then it has the form, $f_L(x_i(r, c)) = a \cdot x_i(r, c) + b$, where a and b are constants. Let $u = x_i(r, c)$ be the gray-scale value of the image, then this equation can be rewritten as, $f_L(u) = a \cdot u + b$. Examples of linear functions are image equalization and image inversion.

By definition, an injective function is a one-to-one mapping function, such that,

$$\mathfrak{S}(u) = \{\mathfrak{S}(u) \in \mathfrak{R} \mid \mathfrak{S}(u_1) \neq \mathfrak{S}(u_2), u_1, u_2 \in \mathfrak{R}\} \quad (18)$$

or $\mathfrak{S}^{-1}(\mathfrak{S}(u)) = u$, i.e. each value $u \in \mathfrak{R}$ maps to a unique value in \mathfrak{R} . Consequently an injective transform acting on image \mathbf{x}_1 producing image \mathbf{x}_2 maps each intensity value of \mathbf{x}_1 into a unique intensity value in \mathbf{x}_2 . Hence, the linear function, f_L , defined above is an injective function if, $a \cdot u_{\max} + b \leq 2^n$ or $\log_2(a \cdot u_{\max} + b) \leq n$, where u_{\max} is the maximum intensity value of the input image and n is the number of bits used to represent the image. Injective functions are not restricted to linear functions but can also be non-linear. For example, the non-linear function $f_N(u) = u^m$ is an injective function if $(u_{\max})^m \leq 2^n$ or $m \cdot \log_2(u_{\max}) \leq n$.

3.1. Injective and Reversible Processes

The second law of thermodynamics, also known as the increase of entropy principle, states that “the entropy of an isolated system during a process always increases or, in the limiting case of a reversible process, remains constant” [9]. Since all processes in nature involve some energy loss due to friction or heat dissipation -which decreases the amount of system order- reversible thermodynamic systems simply do not exist in nature, they are only used as a theoretical idealization of the process. If such a reversible system was to exist, the change of

system entropy must be zero ($\Delta E = 0$), and the entropies of the initial and final states of the system must be equal ($E_i = E_f$, where i and f denote the initial and final states of the process, respectively).

In image analysis, this is not the case. We can have images that are processed by a reversible or injective transform, where the image entropy remains unchanged and the entropy of the transformed image equals that of the original image. This is evident by examining the histograms of an image and its injective transformed image. Fig. 1 shows the histogram distribution of an image and the effect of five transforms on the original histogram distribution. The first three transforms are injective transforms while the remaining two are not. It is fairly obvious that the first two transforms (image inversion and equalization) produce images that have the same histogram distribution profile as the original histogram, but in reverse order for the first case and stretched in the second case. The third transform also produces the same histogram but is difficult to see because the order of the histogram has been scrambled. However, all histogram values are 100% preserved. The remaining two transforms clearly produced different histogram profiles. What occurs as a result of an injective transform, is merely a change in the order of the histogram

distribution, i.e. $h_i(\mathbf{x}) = h_{r(i)}(\mathfrak{S}(\mathbf{x}))$, where $r(i)$ is the histogram order index for the transformed image. All histogram values are preserved and not modified by such a transform. Hence, $\Delta E = 0$ or $E_i = E_f$. This fact implies that the change in the image variation number is also zero ($\Delta \Pi = 0$), and that $\Pi_i = \Pi_f$. This can be shown to be true by,

$$\Pi(\mathfrak{S}(\mathbf{x})) = \sum_{i=0}^{L-1} \delta(h_{r(i)}(\mathfrak{S}(\mathbf{x}))) = \delta(h_{r(i)}(\mathfrak{S}(\mathbf{x}))) = \Pi(\mathbf{x}) \quad (19)$$

3.2. The Injectiveness Theorem

Although $\Delta \Pi = 0$ (or $\Delta E = 0$) is a necessary condition to identify if a transform between two images is an injective transform, it is not a sufficient condition. Many images

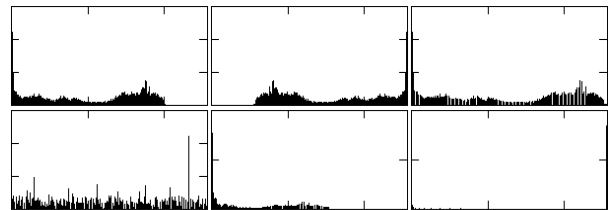


Fig. 1. Histogram distributions for the *Phone* Image. From left to right. Top row: original image, image inversion and image equalization. Bottom row: random intensity mapping, squared intensity mapping with normalization, and squared intensity mapping with clipping.

can be found where they have the same values of Π or E . Does this mean that one image can be obtained from the other image by an injective function? Certainly not. As we state in the injectiveness theorem below, the joint variation number of the two images must also equal the image variation number of each image for an injective transform to exist between two images.

Injectiveness Theorem

Given two images \mathbf{x}_1 and \mathbf{x}_2 . If,

$$\Pi(\mathbf{x}_1, \mathbf{x}_2) = \Pi(\mathbf{x}_1) = \Pi(\mathbf{x}_2) \quad (20)$$

then the mapping $\mu: \mathbf{x}_1 \leftrightarrow \mathbf{x}_2$ is an injective (one-to-one) mapping.

Proof. Let $\Pi(\mathbf{x}_1, \mathbf{x}_2) = \Pi(\mathbf{x}_1) = \Pi(\mathbf{x}_2) = L$. $\Pi(\mathbf{x}_1, \mathbf{x}_2) = L$ implies that the number of non-zero entries in their GCT is L . Hence, the mapping between \mathbf{x}_1 and \mathbf{x}_2 has L distinct gray-scale intensity pairs. Furthermore, since each image has only L distinct intensity values also, this means that each intensity value of \mathbf{x}_1 has a unique intensity value of \mathbf{x}_2 and vice-versa.

Note that both images \mathbf{x}_1 and \mathbf{x}_2 must be of equal size for the injective theorem to be applicable.

3.3. Recovering Injective Transforms

Once a transform between two images has been determined to be injective, the transform itself can be recovered by examining the GCT of the two images. As stated above, the GCT can be interpreted as a two dimensional mapping matrix that indicates the gray-scale intensity correspondence between two images. Hence, simple curve fitting techniques can be used to fit the GCT mapping to obtain the functional relation between two images. For example, the first two GCT plots shown in Fig. 4 are easily identified as linear mapping functions, and using simple line fitting techniques we can reproduce the mapping function. The third GCT plot of Fig. 4 is also injective, although it is more difficult to identify. Here, no explicit mapping equation can be stated as it is a result of a random injective mapping, but a correspondence LUT can be easily constructed. The fourth GCT plot of Fig. 4 is easily identified as a parabolic function and the GCT data can be fitted to a parabolic equation to arrive at the mapping equation, and so on.

3.4. Mapping Indexes

Image transforms are either injective or not. Using the Injectiveness Theorem we can determine if the transform is an injective transform. However, some transforms are not injective but may have some common attributes of injective transforms because of their closeness to being injective transforms. By using the two indexes defined below we can determine the transform's degree of nearness to an injective transform. Before presenting the

two measures, recall the calculus definition of a mathematical *function*: "Let X and Y be non-empty sets. Let f be a collection of ordered pairs (x,y) with $x \in X$ and $y \in Y$. Then f is a function from X to Y if to every $x \in X$ there is assigned a **unique** $y \in Y$ " [10].

Injective Mapping Index. The injective mapping index (F_Δ) between two images, \mathbf{x}_1 and \mathbf{x}_2 , is defined as,

$$F_\Delta(\mathbf{x}_1, \mathbf{x}_2) = 1 - \frac{\sqrt{(\Pi(\mathbf{x}_1, \mathbf{x}_2) - \Pi(\mathbf{x}_1))^2 + (\Pi(\mathbf{x}_1, \mathbf{x}_2) - \Pi(\mathbf{x}_2))^2}}{\sqrt{2} \cdot \Pi(\mathbf{x}_1, \mathbf{x}_2)} \quad (21)$$

which represents the closeness of a transform or a mapping between two images being injective. The range of $F_\Delta(\mathbf{x}_1, \mathbf{x}_2)$ is $[0,1]$. $F_\Delta(\mathbf{x}_1, \mathbf{x}_2) = 1$ indicates an injective mapping function between \mathbf{x}_1 and \mathbf{x}_2 , which is bi-directional between the two images. Large values of F_Δ indicate closeness of the mapping being injective.

Functional Mapping Index. The functional mapping index (F_μ) between two images, \mathbf{x}_1 and \mathbf{x}_2 , is defined as,

$$F_\mu(\mathbf{x}_1, \mathbf{x}_2) = \max(\Pi(\mathbf{x}_1), \Pi(\mathbf{x}_2)) / \Pi(\mathbf{x}_1, \mathbf{x}_2) \quad (22)$$

It indicates the closeness of the transform from $\mathbf{x}_s \rightarrow \mathbf{x}_t$ being a function, where,

$$\mathbf{x}_s = \{\mathbf{x}_i \mid \Pi(\mathbf{x}_i) = \min(\Pi(\mathbf{x}_1), \Pi(\mathbf{x}_2))\}$$

$$\mathbf{x}_t = \{\mathbf{x}_i \mid \Pi(\mathbf{x}_i) = \max(\Pi(\mathbf{x}_1), \Pi(\mathbf{x}_2))\} \quad (23)$$

The range of $F_\mu(\mathbf{x}_1, \mathbf{x}_2)$ is $[0,1]$ where $F_\mu(\mathbf{x}_1, \mathbf{x}_2) = 1$ indicates a unidirectional mapping function from $\mathbf{x}_s \rightarrow \mathbf{x}_t$. For any two images, $F_\mu(\mathbf{x}_1, \mathbf{x}_2) \geq F_\Delta(\mathbf{x}_1, \mathbf{x}_2)$. $F_\Delta(\mathbf{x}_1, \mathbf{x}_2) = 1$ implies that $F_\mu(\mathbf{x}_1, \mathbf{x}_2) = 1$, but the converse is not true.

4. Applications

Thirty images were employed for testing the injectiveness theorem and the mapping indexes. The test images were randomly selected from our image database which consists of more than 100 images. The images are 8-bit gray-scale images of size 128x128. Values of the variation number (Π) for the test images varied from 14 to 255 for the image set with a median set value of 192. These images were point processed by the following five functions: f_1 : image inversion: $f(x) = 255 - x$, f_2 : image equalization, f_3 : random intensity mapping: $f(x) = \text{random}(x)$, such that $f(x_1) \neq f(x_2)$, f_4 : squared intensity mapping with normalization: $f(x) = x^2/255$, $f(x) = [0,255]$ and f_5 : squared intensity mapping with clipping: $f(x) = x^2$, and $f(x) = 255$ if $f(x) > 255$. f_1 and f_3 are injective functions. f_2 is also an injective function provided that the image can be equalized. f_4 may or may not be an injective function. f_5 is an injective function only if $\Pi < 16$. Fig. 2 and Fig. 3 show two sample images, the

Phone image and the Fires image, along with their transformed images.

The processed images resulting from applying $f_1 - f_5$ to the original images were pooled together with the original images, denoted by f_0 , and used as the test set. This resulted in 178 images as two images could not be equalized. Every pair of images were then examined to see if the injectiveness theorem is satisfied. This resulted in the calculation of the joint variation number for 31,684 image pairs, of which 119 image pairs were found to satisfy the injectiveness theorem ($F_{\Delta} = 1$). Each image and its transformed images by $f_1 - f_3$ successfully satisfied the injectiveness theorem. Only one image ($\Pi(f_0) = 14$) had its f_5 transformed image satisfying the injectiveness theorem.

4.1. Mapping Results

In our discussion we will analyze the results for two sample images, the *phone* image and the *fires* image and discuss their results. The image set for the *phone* image consists of 6 images: the original image and its transformed images $\{f_i(x_{phone}) | i = 0, \dots, 5\}$. The histogram distribution for these images were earlier shown in Fig. 1. The image set for the *fires* image consists of 5 images: $\{f_i(x_{fires}) | i = 0, 1, 3, 4, 5\}$ as this image could not be

equalized. Hence, the joint image set for these images consists of 11 images. Tables 1 and 2 display the injective mapping index (F_{Δ}) and the functional mapping index (F_{μ}) for all 121 possible image pairs. Fig. 4 displays a plot of the *GCT* for several image pairs.

4.1.1. Phone-Phone image Pairs. Each image pair of the subset $\{f_i(x_{phone}) | i = 0, \dots, 3\}$ produced $F_{\Delta} = 1$ (and $F_{\mu} = 1$), indicating an injective transform for all pairs of this subset. Also all image pairs of the *Phone-Phone* image pairs had very high F_{μ} values (≥ 0.9). In fact all pairs -except one- had $F_{\mu} = 1$, indicating that all image pairs except one image pair has one-to-one mapping correspondence from one of the images to the other. This is an important finding since even though some image pairs do not have an injective mapping between them, one image can still be produced from the other by a mathematical function (algebraic or LUT).

4.1.2. Fires-Fires image pairs. Each image pair of the subset $\{f_i(x_{fires}) | i = 0, 1, 3\}$ produced $F_{\Delta} = 1$ (and $F_{\mu} = 1$), indicating an injective transform for all pairs of this subset. In general, all image pairs in this set had very high F_{μ} values (≥ 0.87). All pairs -except one- had $F_{\mu} = 1$, indicating that all image pairs except one image pair has one-to-one mapping correspondence from one of the images to the other.

Table 1: Injective Mapping for *phone* and *fires* Images

Image	$x = phone$						$y = fires$					
	f_0	f_1	f_2	f_3	f_4	f_5	f_0	f_1	f_3	f_4	f_5	
x	f_0	1.00	1.00	1.00	1.00	0.78	0.35	0.02	0.02	0.02	0.03	0.05
	f_1	1.00	1.00	1.00	1.00	0.78	0.35	0.02	0.02	0.02	0.03	0.05
	f_2	1.00	1.00	1.00	1.00	0.78	0.35	0.02	0.02	0.02	0.03	0.05
	f_3	1.00	1.00	1.00	1.00	0.78	0.35	0.02	0.02	0.02	0.03	0.05
	f_4	0.78	0.78	0.78	0.78	1.00	0.37	0.02	0.02	0.02	0.03	0.05
	f_5	0.35	0.35	0.35	0.35	0.37	1.00	0.06	0.06	0.06	0.06	0.08
y	f_0	0.02	0.02	0.02	0.02	0.02	0.06	1.00	1.00	1.00	0.76	0.42
	f_1	0.02	0.02	0.02	0.02	0.02	0.06	1.00	1.00	1.00	0.76	0.42
	f_3	0.02	0.02	0.02	0.02	0.02	0.06	1.00	1.00	1.00	0.76	0.42
	f_4	0.03	0.03	0.03	0.03	0.03	0.06	0.76	0.76	0.76	1.00	0.43
	f_5	0.05	0.05	0.05	0.05	0.05	0.08	0.42	0.42	0.42	0.43	1.00

Table 2: Functional Mapping for *phone* and *fires* Images

Image	$x = phone$						$y = fires$					
	f_0	f_1	f_2	f_3	f_4	f_5	f_0	f_1	f_3	f_4	f_5	
x	f_0	1.00	1.00	1.00	1.00	1.00	1.00	0.03	0.03	0.03	0.05	0.10
	f_1	1.00	1.00	1.00	1.00	1.00	1.00	0.03	0.03	0.03	0.05	0.10
	f_2	1.00	1.00	1.00	1.00	1.00	1.00	0.03	0.03	0.03	0.05	0.10
	f_3	1.00	1.00	1.00	1.00	1.00	1.00	0.03	0.03	0.03	0.05	0.10
	f_4	1.00	1.00	1.00	1.00	1.00	0.90	0.03	0.03	0.03	0.05	0.09
	f_5	1.00	1.00	1.00	1.00	0.90	1.00	0.10	0.10	0.10	0.10	0.09
y	f_0	0.03	0.03	0.03	0.03	0.03	0.10	1.00	1.00	1.00	1.00	1.00
	f_1	0.03	0.03	0.03	0.03	0.03	0.10	1.00	1.00	1.00	1.00	1.00
	f_3	0.03	0.03	0.03	0.03	0.03	0.10	1.00	1.00	1.00	1.00	1.00
	f_4	0.05	0.05	0.05	0.05	0.05	0.10	1.00	1.00	1.00	1.00	0.82
	f_5	0.10	0.10	0.10	0.10	0.09	0.09	1.00	1.00	1.00	0.82	1.00



Fig. 2. Processed Image for *Phone* Image (From left to right): original image, image inversion, random intensity mapping, image equalization, squared intensity mapping with normalization, and squared intensity mapping with clipping.

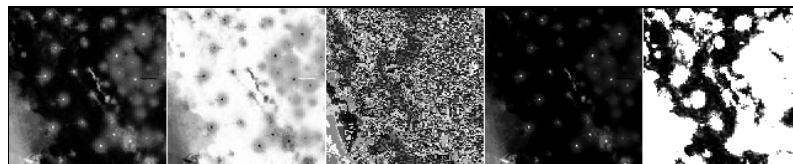


Fig. 3. Processed Image for *Fires* Image (From left to right): original image, image inversion, random intensity mapping, squared intensity mapping with normalization, and squared intensity mapping with clipping (note: image could not be equalized).

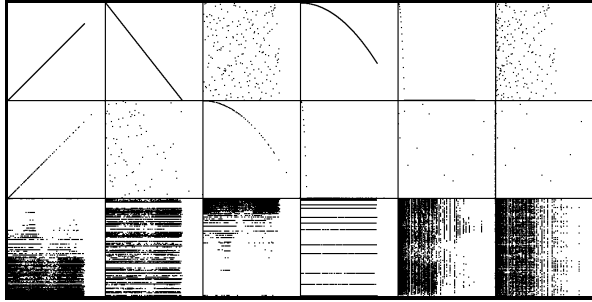


Fig. 4. GCT for the phone and fires images ($x = \text{phone image}$ and $y = \text{fires image}$). From left to right: Top row: $f_0(x)$ & $f_1(x)$, $f_0(x)$ & $f_2(x)$, $f_0(x)$ & $f_3(x)$, $f_0(x)$ & $f_4(x)$, $f_0(x)$ & $f_5(x)$, $f_4(x)$ & $f_3(x)$. Middle row: $f_0(y)$ & $f_1(y)$, $f_0(y)$ & $f_3(y)$, $f_0(y)$ & $f_4(y)$, $f_0(y)$ & $f_5(y)$, $f_5(y)$ & $f_3(y)$, $f_4(y)$ & $f_1(y)$. Bottom row: $f_0(x)$ & $f_1(y)$, $f_0(x)$ & $f_3(y)$, $f_0(x)$ & $f_4(y)$, $f_0(x)$ & $f_5(y)$, $f_0(y)$ & $f_2(x)$, $f_0(y)$ & $f_3(x)$.

4.1.3. The fires-Phone image pairs. In contrast with the results indicated above, the mapping indexes were very small values (≤ 0.1) when the images belong to different image sets, indicating no relation between these images and hence are not -and can not- be produced from each other.

4.2. Transform Recovery

All image pairs producing injective or functional mappings can have their transform equation recovered. For example,

- Fitting the GCT data for the image pair $\{f_0(\mathbf{x}_{\text{phone}}), f_1(\mathbf{x}_{\text{phone}})\}$ produced the equation, $f(x) = 255 - x$, which is the equation for inverting the image.
- Fitting the GCT data for the image pair $\{f_0(\mathbf{x}_{\text{phone}}), f_2(\mathbf{x}_{\text{phone}})\}$ produced the equation, $f(x) = 0.788x + 0.384$, which is the equation for equalizing this image.
- Fitting the GCT data for the image pair $\{f_0(\mathbf{x}_{\text{phone}}), f_3(\mathbf{x}_{\text{phone}})\}$ produced a lookup table that maps each value of $f_0(\mathbf{x}_{\text{phone}})$ to a unique value in $f_3(\mathbf{x}_{\text{phone}})$.
- Fitting the GCT data for the image pair $\{f_0(\mathbf{x}_{\text{phone}}), f_4(\mathbf{x}_{\text{phone}})\}$ -although not a result of an injective transform ($F_\Delta = 0.78$) but of a functional mapping ($F_\mu = 1$) from $f_0(\mathbf{x}_{\text{phone}}) \rightarrow f_4(\mathbf{x}_{\text{phone}})$ - to a second order equation produces the transform equation, $f(x) = 0.003903x^2$, which is in agreement with f_4 (error $< 0.5\%$). Although one might be tempted to state that the function $\sqrt{x / (0.003903)}$ is the mapping of $f_4(\mathbf{x}_{\text{phone}}) \rightarrow f_0(\mathbf{x}_{\text{phone}})$, and that the transform is an injective function, this is not the case, as this last function does not produce $f_0(\mathbf{x}_{\text{phone}})$.

5. Conclusion

In this paper we have presented a novel technique that can identify injective transform image pairs. The injective

mapping function is also recovered in the process. The technique is based on using the joint image variation number, a new entropy-similar information measure. Two mapping indexes, the injective mapping index and the functional mapping index, are used to identify the nearness of a transform to being an injective mapping or a functional mapping, respectively. Tests were successfully conducted on 178 image variations from 30 images, resulting in more than 31,000 image pairs. Using the injectiveness theorem and the mapping indexes the system correctly identified all injective transformed image pairs, and identified all image pairs than can be produced by a direct application of a function to one of the image pairs. Even when applying a random injective transform to an image producing an image with no visible relation to the original image, the method easily detected the two images as being an injective transformed image pair. In each case where an injective transform pair or a functional transform pair was identified the transform function was recovered. It is hoped that the framework laid in this work will assist other researchers in the area of image recovery and restoration.

Acknowledgment. The author would like to thank the Kuwait University Research Administration for providing financial support for this research (Grant EM-05/01).

6. References

- [1] Gonzalez, R. and Woods, R. 1992. *Digital Image Processing*. Addison-Wesley, New York.
- [2] Jain, Anil K. 1989. *Fundamentals of Digital Image Processing*. Prentice Hall, New Jersey.
- [3] Sonka, M., Hlavac, V. and Boyle, R. 1998. *Image Processing, Analysis and machine Vision*. PWS Publishing, New York.
- [4] Ballard, D. and Brown, C., 1982. *Computer Vision*. Prentice Hall, New Jersey.
- [5] Castleman, Kenneth. 1997. *Digital Image Processing*, Prentice-Hall, Inc. New Jersey.
- [6] M. Holz, K. Podewski and K. Steffens. 1987. *Injective Choice Functions*. Lecture Notes in Mathematics, Springer-Verlag, Hannover, Germany.
- [7] Mustafa, Adnan A. 2001. "The Image Variation Number, a Substitute for Image Entropy". Kuwait University, Dept. of Mechanical Engineering, Technical Report #EMM-05/01.
- [8] Cover, T. and Thomas, J. 1991. *Elements of Information Theory*, John Wiley & Sons. New York.
- [9] Yunis, C. and Boles, M. 1998. *Thermodynamics: An Engineering Approach*, 3rd ed., WCB/McGraw Hill, New York.
- [10] Thomas, George B. 1972. *Calculus and Analytical Geometry*, 4th ed., Addison-Wesley, The Philippines.